



euronoise

**Acoustics'08
Paris**
June 29-July 4, 2008

www.acoustics08-paris.org

Modal analysis of resonances of an elliptic elastic cylinder immersed in water

Fernand Leon^a, Farid Chati^a and Jean-Marc Conoir^b

^aLOMC FRE 3102 CNRS Groupes Ondes Acoustiques, Université du Havre (IUT), Place Robert Schuman, 76610 Le Havre, France

^bInstitut Jean Le Rond d'Alembert-UMR CNRS 7190, Université Paris 6, tour 55-65, 4 place Jussieu, 75005 Paris, France
farid.chati@univ-lehavre.fr

Considerable work has been done on the scattering by cylindrical objects having a circular cross section. The modal formalism based on the theory of elasticity has been developed for studying the acoustic scattering by these elastic cylinders immersed in water. In particular, it has been demonstrated, in normal incidence, that the eigenfrequencies of a circular cylinder can be determined from a resonance spectrum. These eigenfrequencies correspond to circumferential waves that form a resonance when a phase matching along a closed path is obtained. Each eigenfrequency is characterized by a given mode n , i.e., the number of wavelengths spanning the circumference. Comparatively, little attention has been devoted to the more general case of the noncircular cylindrical cylinders such as the elliptical elastic cylinders. For these objects, we have been developed a modal formalism based on the theory of elasticity. From the results obtained theoretically and experimentally, we show how to obtain a resonance spectrum, independently of the azimuth incident angle and of the radii ratio (minor radius and major radius) so that the eigenfrequencies can be determined. We present also a modal analysis of resonances as function of the azimuth incident angle and of the radii ratio.

1 Introduction

Considerable work has been done on the scattering by cylindrical objects having a circular cross section. A large amount of literature devoted to this topic can be found in Ref. 1. Comparatively, little attention has been given to the more general case of the noncircular cylindrical cylinders. Experimental results are even fewer for this type of scatterers [2,3]. The aim of our paper is to obtain, theoretically and experimentally, the resonance spectrum of an elliptical elastic cylinder immersed in water and then, by considering a modal formalism, to determine the modes of resonances.

2 Formulation of the problem

The modal formalism presented in reference 4 is used in our paper. Displacement and stress fields in the noncircular cylinder are directly expressed in terms of modal series as for the incident and scattered fields. The difficulty consists in writing the boundary conditions and in calculating the unknown scattering coefficients A_n . The way of circumventing this difficulty is to expand all the fields in trigonometric series. The linear system of equations obtained finally can be solved numerically.

The noncircular cylindrical cylinders considered here is an elliptical aluminum cylinder. Experimental and Numerical results are presented for a plane wave incidence normal to the axis of this cylinder. In the cylindrical coordinates system (r, θ, z) , the cylinder radius is expressed as follows

$$r(\theta) = a \left[\cos^2 \theta + \left(\frac{a}{b} \right)^2 \sin^2 \theta \right]^{1/2}, \quad (1)$$

where a is the major radius and b is the minor one. This solid is characterized by the following parameters: density $\rho_2 = 2765 \text{ kg/m}^3$, longitudinal wave speed $C_L = 6440 \text{ m/s}$, shear wave speed $C_T = 3113 \text{ m/s}$, axis ratio $b/a = 0.75$, major radius $a = 2 \text{ cm}$. This aluminum cylinder is immersed in water ($C_1 = 1470 \text{ m/s}$, $\rho_1 = 1000 \text{ kg/m}^3$).

The interaction of an ultrasonic harmonic plane wave with an elastic cylinder is described in permanent regime, by a modal representation (Rayleigh series) [4]. Thus, the expression of the pressure field scattered by the object

$P_S(r, \theta, \omega)$ at a point of observation (r, θ) is developed into a series of normal modes

$$P_S(r, \theta) = \sum_{n=-\infty}^{+\infty} i^n A_n H_n^{(1)}(kr) e^{i n \theta}, \quad (2)$$

and is approximated in far field, as follows

$$P_S(r, \theta) \approx P_{S0}(\theta) e^{ikr},$$

$$P_{S0}(\theta) \approx \sqrt{2/(\pi kr)} e^{-i\pi/4} \sum_{n=-\infty}^{+\infty} A_n e^{i n \theta} = \sum_{n=-\infty}^{+\infty} P_{S0n}, \quad (3)$$

where $k = \omega / C_1$ ($f = \omega / (2\pi)$) denotes the wave number of the incident wave, ω the pulsation and C_1 the sound speed in the fluid. $H_n^{(1)}$ is the first Hankel function of order n . A_n is the unknown scattering coefficient determined from the boundary conditions.

3 Experiment and comparison with theory

The short-pulse monostatic and bistatic set-ups of the MIIR [5,6] (method of isolation and identification of resonances) are used to obtain experimental results presented in this paper. The elliptical aluminum cylinder is vertically immersed in a water-filled tank, 3 m in diameter and 2 m deep. The aspect ratio b/a of the elliptical cylinder is equal to 3/4, its length is 20 cm and the major axis radius a is equal to 2 cm. The material properties are the same ones of the previous paragraph. The transducers we used are Panametric V3507 broadband transducers with a central frequency equal to 200 kHz. The central frequency corresponds to $ka=17.1$ in reduced frequency. These transducers allow us to analyze the acoustic scattering in the 100–350 kHz frequency range ($8.5 < ka < 30$) and the diameter of their radiating surfaces is 50 mm.

A short electric pulse is converted into bulk acoustic wave by the emitter transducer. The time-domain responses of the insonified cylinder consist of echo waveforms made up of specular reflections and elastic wave reradiations. In the present investigation, backscattered spectra are obtained with a single transducer (monostatic set-up) from the FFT of time-domain responses. This transducer is used alternately as an emitter and a receiver to obtain the acoustic signature of the cylinder at given incidences. A correction of the passbands of the transducers is then made (Fig.1).

The bistatic set-up enables experimental determination of angular diagrams. Two transducers are used. The emitter transducer is fixed at a given position while the receiver transducer rotates in the azimuthal plane, normally to the cylinder axis. Figure 2 is an example of an angular diagram obtained from this experimental set-up.

The above theoretical formalism constitutes an exact solution for the scattering of a plane wave from a noncircular cylindrical cylinder insonified normal to its axis. Far-field acoustic scattering amplitudes from such elliptical cylinder, calculated for incidences equal to 0°, are shown in Fig. 1. This form function is expressed as follows :

$$f_{\infty} = \sqrt{2 r a_{\text{eff}} / a^2} \left| \frac{P_s}{P_{\text{inc}}} \right| = \sum_{n=-\infty}^{+\infty} f_{\infty n}, \quad (4)$$

where $a_{\text{eff}} = \sqrt{1/2 (a^2 + b^2)}$.

An incident angle is defined for this object because of its nonaxial symmetry. Hence, an incidence equal to 0° corresponds to the angle that the acoustic beam makes with the major axis of the ellipse. The agreement between theory and experiment is very good, validating the theoretical approach presented in this paragraph. This excellent agreement is also noted for angular results obtained at a particular frequency (Fig.2).

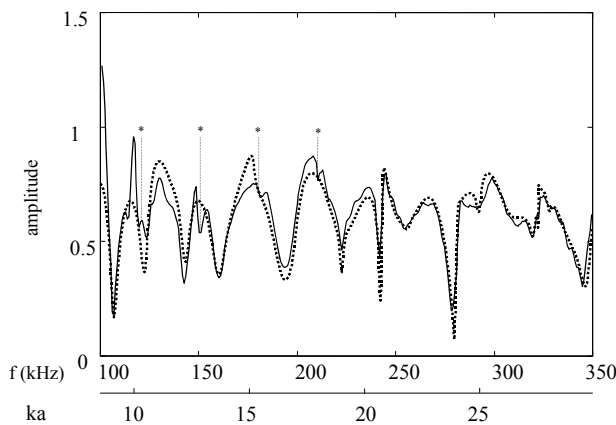


Fig.1 Far field form function of the elliptical aluminum cylinder $\theta_{\text{inc}}=\theta_{\text{rec}}=0^\circ$: theoretical in dotted line, experimental in solid line

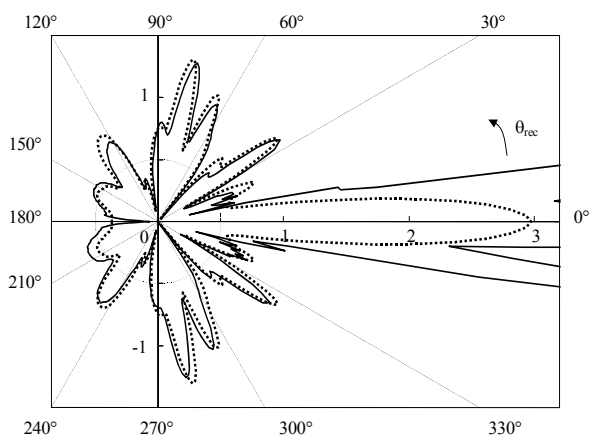


Fig.2 Angular diagram of the elliptical aluminum cylinder at the frequency $f=222.5$ kHz, $\theta_{\text{inc}}=0^\circ$: theoretical in dotted line, experimental in solid line

4 Resonance spectrum

Experimentally and theoretically, it is easy to determine a resonance spectrum of a circular cylinder from a backscattered time signal. For this, it is necessary to eliminate the first echo related to the specular signal and after, to achieve a FFT of the part of signal related to the resonant echoes. A resonance spectrum is thus obtained. For a non-circular cylinder, this process is not obvious to apply because the elliptical cylinder is not axisymmetric. For this, we determine experimental and theoretical resonance spectra by using the frequential derivative of the curvilinear abscissa s . This derivative versus frequency writes in the following way:

$$\frac{ds}{d(ka)} = \sqrt{\left(\frac{d\text{Re}(ka)}{d(ka)}\right)^2 + \left(\frac{d\text{Im}(ka)}{d(ka)}\right)^2} \quad (5)$$

where $\text{Re}(ka) + i \text{Im}(ka) = \sqrt{2 r a_{\text{eff}} / a^2} P_{S0}(\theta)$ and

an effective radius a_{eff} defined by $a_{\text{eff}} = \sqrt{(a^2 + b^2)/2}$.

The frequential derivative of the curvilinear abscissa s reaches a maximal value at a resonance frequency [7]. The knowledge of the non-resonant pressure called background is not necessary because its variations can always be neglected in comparison with those of the resonant pressure when using the derivative of the curvilinear abscissa.

Let us consider for example the case of an aluminum circular solid cylinder. Applying the relation Eq.(5) gives the theoretical resonance spectrum of the figure 3. Each peak of this spectrum corresponds with a resonance. Their physical origin lies in the excitation of surface waves on the cylinder which, for an acoustic signal incident normally to the cylinder axis, circumnavigate the cylinder in a peripheral fashion along a closed circumferential path. If upon each circumnavigation these waves match phases with themselves at their point of origin, this lead to a resonance in the scattering amplitude. Consequently, a circumferential standing wave is formed with an integer number of wavelengths n spanning the circumference [8,9]. The mode of vibration n of each peak of resonance can be determined experimentally with bistatic scattering measurements [6]. Theoretically, the relation Eq.(5) applied to the modal pressure field P_{S0n} (Eq.(3)) enables us to separate each modal contribution (Fig.4). The various resonances represented by a black spot (amplitude) on the interpolated image of the figure 4 are attributed to $\ell = 2, 3, 4, 5$ and 6.

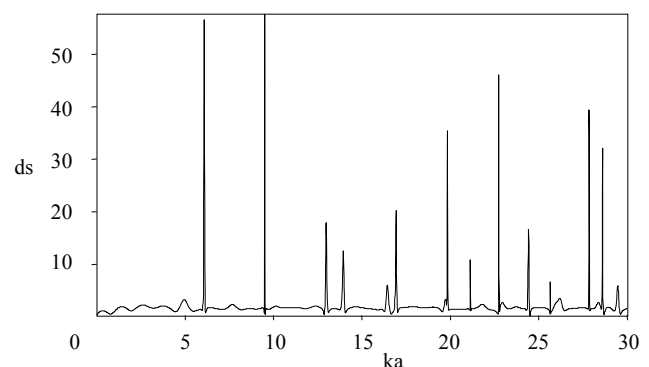


Fig.3 Theoretical backscattered resonance spectrum of a circular solid cylinder

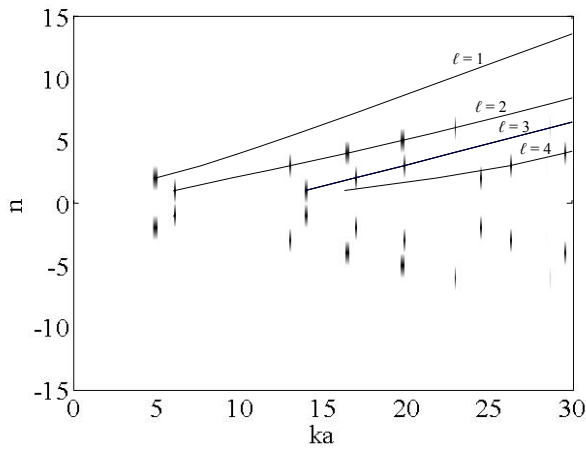


Fig.4 Interpolated image of modal resonance spectra ($-15 \leq n \leq 15$) of a circular solid cylinder

Solid lines are superimposed on figure 4. These lines (Regge trajectories) are plotted from the eigenfrequencies corresponding to circumferential waves, obtained for a circular solid cylinder using the classical elasticity theory [1]. Each resonance can thus be labeled with two integers (ℓ, n). The mode of vibration $|n|$ is the number of wavelengths around the circular cylinder. The parameter ℓ labels the resonances for each mode as the frequency increases.

5 Resonance spectra of elliptical cylinder

Theoretically and experimentally, the backscattered resonance spectrum enables us to obtain the acoustic signature of the cylinder at given incidences [10]. Contrary to the circular cylinder, a significant dependence on incident angle θ_{inc} is noted on Fig.5 and Fig.6. Experimental results are compared with the predictions made using dotted lines. A good agreement is noted. Nevertheless, some differences pointed out by asterisks can be observed in the low frequency part of the resonance spectra, particularly in the case of a radial symmetry (Fig.6, $\theta_{inc} = 90^\circ$). Peaks on the experimental curve are not visible on the theoretical one. These peaks, which are regularly spaced, are very certainly due to the resonances of guided waves. They can be experimentally observed because of the directivity of the transducers and the limited length of the cylinder ($L=200$ millimeters). The interpretation of these peaks can be suggested according to what happens for the acoustic scattering by elastic circular cylinders [11]. The guided waves are SH-polarized helical surface waves excited at oblique incidence only (the wave vector of the incident wave is not perpendicular to the z-axis). This is the reason why the peaks are not observed on the theoretical curve calculated for a normally incident wave.

6 Discussion

The agreement between theory and experiment is good enough to allow the experimental data to be interpreted from our model. The case treated in this paragraph relates to an incidence of 90° .

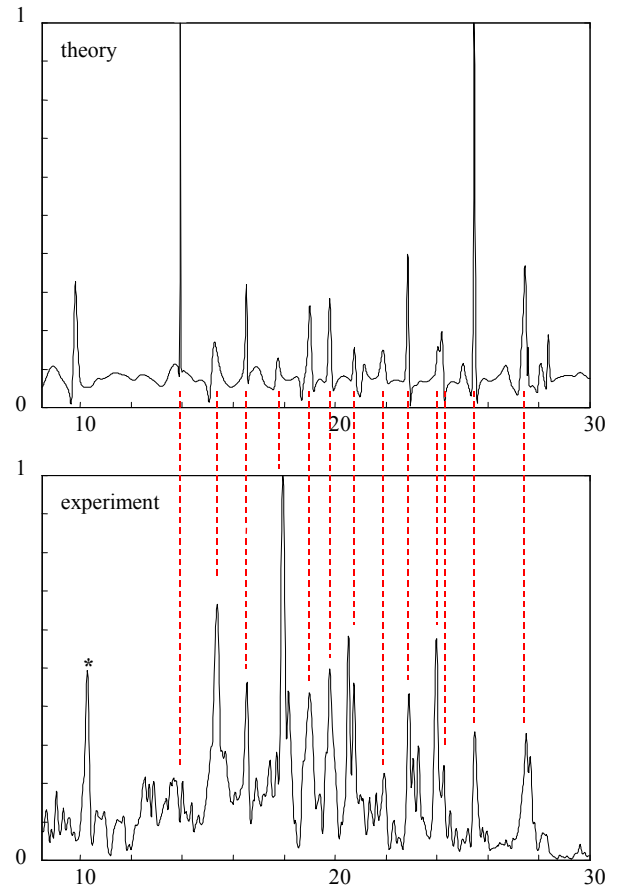


Fig.5 Resonance spectra $\theta_{inc}=45^\circ$ (the transducer bandwidth is not corrected)

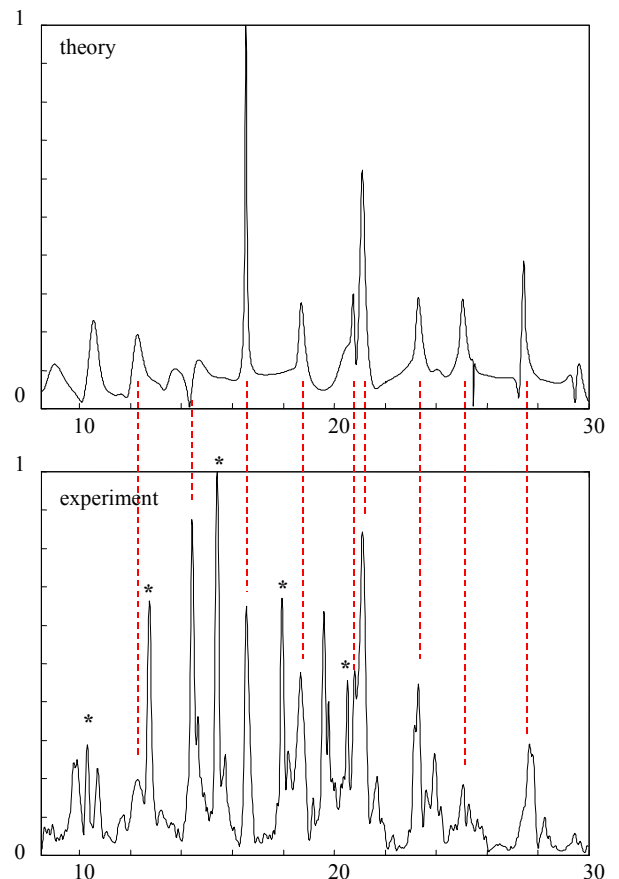


Fig.6 Resonance spectra $\theta_{inc}=90^\circ$ (the transducer bandwidth is not corrected)

In order to show the influence of the axis ratio b/a on the resonances, spectra have been computed for different minor radii b (from $b/a = 1$ to $b/a = 0.75$ with a step equal to 0.01). The results which depend on the axis ratio b/a , are shown in the gray level graph of figure 7 (the darker the shade of gray is, the bigger the amplitude is). This representation enables us to isolate the resonances and to follow them from the circular cylinder ($b/a = 1$) to the elliptical cylinder characterized by $b/a = 0.75$.

As example, let us consider two resonances, close to the central frequency of the transducers. A solid black line surrounds these two resonances on figure 7. For the elliptical cylinder characterized by $b/a=0.75$, the resonance frequencies ka are respectively equal to 16.44 (192.3 kHz) and 18.59 (217.5 kHz). Those are easily observable on the theoretical and experimental resonance spectra of figure 6. On the figure 7, the evolution of the resonance frequencies versus the axis ratio b/a ($b/a=0.75 \rightarrow 1$) shows that for a circular cylinder, the resonance frequencies, $ka=13.95$ and $ka=16.41$ are respectively those of the waves ($\ell=3, n=1$) and ($\ell=2, n=4$). Nevertheless, it is not possible to conclude that the modes of two resonances relating to the elliptical cylinder $b/a=0.75$ are characterized respectively by $n=1$ and $n=4$.

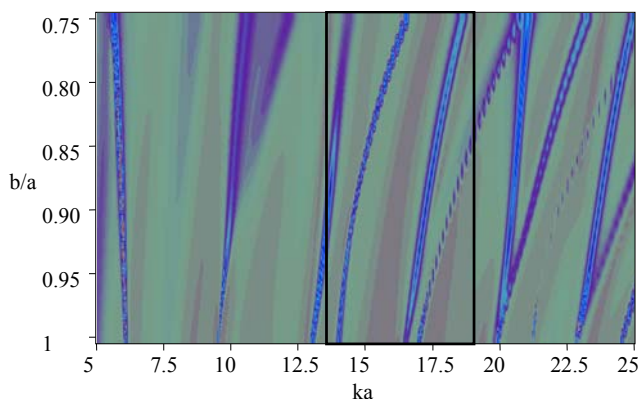


Fig.7 Representation (gray level graph) of theoretical resonance spectra, $\theta_{inc}=90^\circ$, versus b/a (interpolated image)

The gray level graph of figure 8 relating to the modal resonance spectra ($-15 \leq n \leq 15$) of an elliptical cylinder ($b/a=0.75$) shows that the distribution of modes is rather

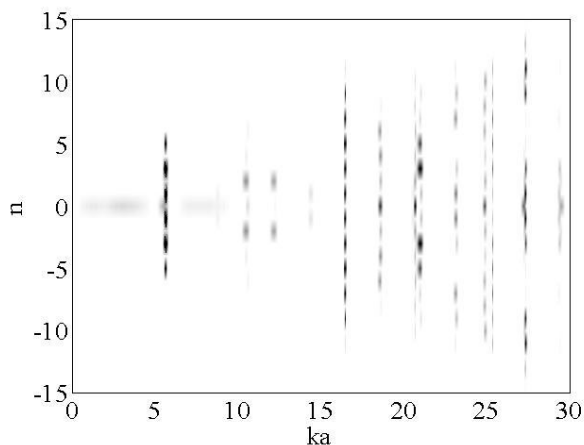


Fig.8 Interpolated image of modal resonance spectra ($-15 \leq n \leq 15$) of an elliptical cylinder ($b/a=0.75$)

confusing. It is not easy to gather together resonances in order to constitute families of wave as the circular cylinder (Fig.4). Moreover, we note that, at a resonance frequency, many more modes are observed than for the circular cylinder.

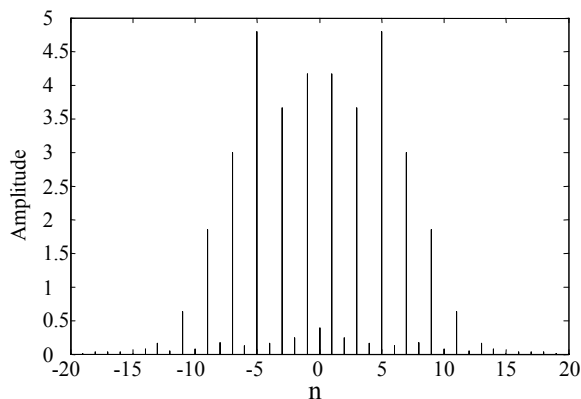


Fig.9a Distribution of modes at $ka=16,44$ for an elliptical cylinder ($b/a = 0.75$)

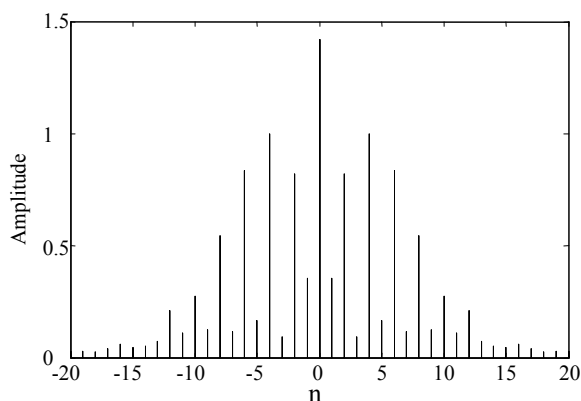


Fig.9b Distribution of modes at $ka=18,59$ for an elliptical cylinder ($b/a = 0.75$)

Fig.9a and Fig.9b are the distribution of modes at the two resonance frequencies previously considered for the elliptical cylinder. It appears, contrary to the circular cylinder (Fig.10a, Fig.10b), that a resonance of the elliptic cylinder is characterized by several modes.

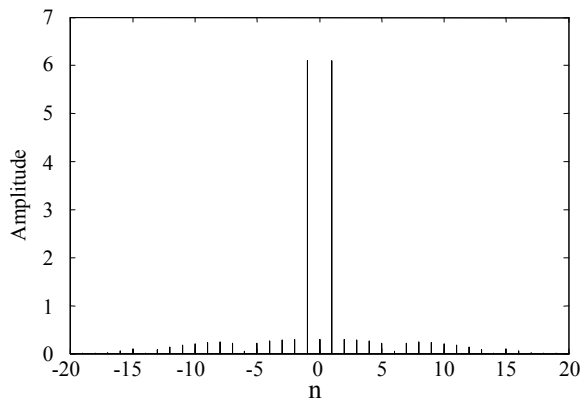


Fig.10a Distribution of modes at $ka=13,95$ for a circular cylinder, wave $\ell=3$, mode of vibration $n= 1$

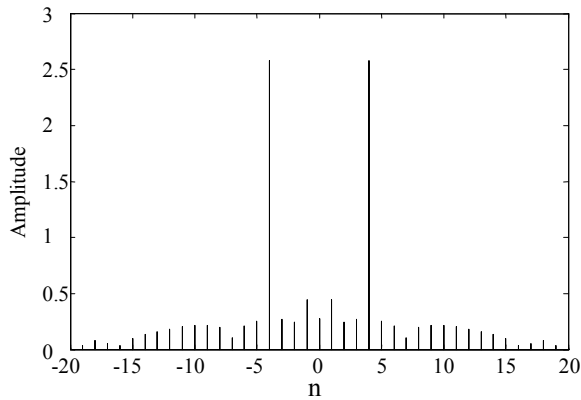


Fig.10b Distribution of modes at $ka=16,41$ for a circular cylinder, wave $\ell=2$, mode of vibration $n=4$

5 Conclusion

A modal formalism based on the theory of elasticity is used to study the acoustic scattering by an elliptical elastic cylinder, insonified normally to the axis of this cylinder. Good agreement with experiment has been obtained with backscattering results.

In order to determine a resonance spectrum independently of the azimuthal incident angle, we apply the frequential derivative of the curvilinear abscissa s to the pressure field scattered by the elliptical cylinder. An identical treatment is applied to the experimental data. The resonance spectrum obtained experimentally shows the presence of additional peaks relating to the guided waves. These waves are generated because of the directivity of the transducers and the limited length of the elliptical cylinder. Despite these additional peaks, the experimental spectra of resonance are in good agreement with the theoretical predictions.

The agreement between theory and experiment enables us to validate the theoretical approach. Then, the frequential derivative of the curvilinear abscissa s is applied also to the modal pressure. Each resonance spectrum obtained depends on the mode n . For a circular cylinder, the resonances are easily isolated, and identified with their mode of vibration. Compared to a circular cylinder, resonances of an elliptic cylinder are identifiable with more difficulty. At a resonance frequency, many more modes are observed than for the circular cylinder.

References

- [1] N.D. Veksler, *Resonant Acoustic Spectroscopy*, Springer-Verlag, Berlin, (1993)
- [2] P.A. Chinnery, V.F. Humphrey, "Fluid column resonances of water-filled cylindrical shells of elliptical cross section", *J. Acoust. Soc. Am.* 103, 1296–1305 (1997)
- [3] A. Pereira, A. Tadeu, and J. Antonio, "Influence of the cross section geometry of a cylindrical solid submerged in an acoustic medium on wave propagation", *Wave Motion* 36, 23–39 (2002)
- [4] F. Léon, F. Chati, J.M. Conoir, "Modal theory applied to the acoustic scattering by elastic cylinders of arbitrary cross section", *J. Acoust. Am. Soc.* 116, 686–692, (2004)
- [5] P. Pareige, P. Rembert, J.L. Izbicki, G. Maze, J. Ripoche, "Méthode impulsionnelle numérisée (MIN) pour l'isolement et l'identification des résonances de tubes immergés", (Digitized Impulse Method (DIM) applied to the isolation and the identification of immersed cylindrical shell resonances) *Physic letters A* 135, 143-146 (1989)
- [6] G. Maze, J. Ripoche, "Méthode d'isolement et d'identification des Résonances (M.I.I.R) de cylindres et de tubes soumis à une onde acoustique plane dans l'eau", (Method of isolation and identification of resonances (M.I.I.R) of cylinders and cylindrical shells insonified by a plane acoustic wave in water), *Rev. Phys. Appl.* 18, 319–326 (1983)
- [7] S. Derible, P. Rembert, J.L. Izbicki, "Experimental determination of acoustic resonance width via the Argand diagram", *Acustica-acta austica*, 84, 270-279 (1998)
- [8] L. Flax, L.R. Dragonette, H. Überall, " Theory of elastic resonance excitation by sound scattering", *J. Acoust. Soc. Am.*, 63, 723-731 (1978)
- [9] H. Überall, L.R. Dragonette, L. Flax, "Relation between creeping waves and normal modes of vibration of a curved body", *J. Acoust. Soc. Am.*, 61, 711-715 (1977)
- [10] R.P. Raddlinski, M.M. Simon, "Acoustic and elastic scattering from elliptic-cylindrical shells", *J. Acoust. Am. Soc.*, 93, 2443-2453 (1993)
- [11] G. Maze, J. L. Izbicki, J. Ripoche, "Resonances of plates and cylinders: guided waves", *J. Acoust. Soc. Am.*, 77, 1352-1357 (1985)